Toxicology Letters 192 (2010) 316–323

Contents lists available at ScienceDirect

Toxicology Letters

journal homepage: www.elsevier.com/locate/toxlet

Expression of glutathione S-transferase M2 in stage I/II non-small cell lung cancer and alleviation of DNA damage exposure to benzo[a]pyrene

Sheau-Chung Tang[a], Gwo-Tarng Sheu[a], Ruey-Hong Wong[b], Chia-Ying Huang[a], Mao-Wen Weng[a], Li-Wen Lee[c], Chung-Ping Hsu[c,d,*], Jiunn-Liang Ko[a,e,*]

[a] Institute of Medical and Molecular Toxicology, Chung Shan Medical University, Taichung, Taiwan, ROC
[b] Department of Public Health, Chung Shan Medical University, Taichung, Taiwan, ROC
[c] Division of Thoracic Surgery, Department of Surgery, Taichung Veterans General Hospital, Taichung, Taiwan, ROC
[d] School of Medicine, National Yang-Ming University, Taipei, Taiwan, ROC
[e] Department of Medical Oncology and Chest Medicine, Chung Shan Medical University Hospital, Taichung, Taiwan, ROC

ARTICLE INFO

Article history:
Received 1 September 2009
Received in revised form 2 November 2009
Accepted 2 November 2009
Available online 10 November 2009

Keywords:
Glutathione S-transferases
NSCLCs
BPDE-DNA adduct
B[a]P
DNA methylation

ABSTRACT

Glutathione S-transferases (GSTs) are a family of inducible enzymes that are important in carcinogen detoxification. GST-Mu class is showing the high activity towards most polycyclic aromatic hydrocarbon (PAH) epoxide. Our objective is to clarify the expression of GST-M2 in non-small-cell lung carcinoma (NSCLC) patients and to determine the role of GST-M2 in protecting against DNA damage. We detected changes in GST-M2 expression at mRNA levels with a panel of lung cell lines and clinical samples of malignant and paired adjacent non-malignant tissues from 50 patients with stage I or II non-small-cell lung carcinoma using real-time RT-PCR. Comet assay and γ-H2AX were used to clarify whether DNA damaged was protected by GST-M2. Our data demonstrate that the expression of GST-M2 in tumor tissues is significantly lower than in paired adjacent non-malignant tissues ($p = 0.016$). Loss of GST-M2 is closely associated with age, gender, *T* value, *N* value and cell differentiation ($p < 0.05$) in early stage I/II patients. Downregulation of GST-M2 is mediated through aberrant hypermethylation in lung cancer cell lines. Protection against B[a]P-induced DNA damage by GST-M2 in lung cancer cells was detected by Comet assay and γ-H2AX. In conclusion, DNA hypermethylation altered and reduced GST-M2 expression that resulted in susceptible to benzo[a]pyrene (B[a]P) induced DNA damage. It implies that GST-M2 reduction occurs prior to tumorigenesis.

1. Introduction

Susceptibility to lung cancer is associated with several environmental factors and xenobiotics, which may be metabolized and detoxified by phase II enzymes, glutathione S-transferases (GSTs). Through exposure to tobacco carcinogenic metabolites, including polycyclic aromatic hydrocarbons (PAHs), the lung is constantly challenged by latent harmful compounds (Kelley et al., 2005). Benzo(a)pyrene (B[a]P), the most extensively studied of the PAHs, is a carcinogen found in cigarette smoke and is considered a cause of lung cancer (Alexandrov et al., 2002), specifically inducing DNA damage (Orlow et al., 2008). B[a]P can be activated to a highly reactive species, benzo(a)pyrene-7,8-diol-9,10-epoxide (BPDE), by cytochrome *P*450 enzyme (phase I enzyme). Through highly mutagenic attack with the N^2 position of guanine residues in DNA-BPDE can form a stable BPDE-N^2-deoxyguanosine (BPDE-dG) adduct, which plays a critical role in tumorigenesis (Alexandrov et al., 2006). The presence of BPDE-DNA adducts in human bronchial cells points to their involvement in induction of mutation in *p53*, and initiation of human lung cancer (Rojas et al., 2004).

The expression levels of the different GSTs are tissue specific (Konig-Greger et al., 2004). Within each of the GST isoforms there are significant differences in substrate specificity (Kearns et al., 2003). GST isoforms have also been found to possess different activities in tissues such as muscle, testis, brain, heart, blood, liver and upper areodigestive mucosa (Hayes and Pulford, 1995; Matthias et al., 1999; Tsuchida et al., 1990). In adult human liver, 80% of the total GST proteins are GST-Alpha members, while the Pi-class enzyme is present in essentially all tissues except the liver (Castro et al., 1990; Mannervik et al., 1987; Shea et al., 1988). In Chinese hamster lung fibroblastoid cell line, the Mu class shows the highest activity towards most PAH epoxides, followed by GST-Pi and GST-Alpha (Sundberg et al., 2002).

GST-M2, a muscle-specific isozyme, occurs only minimally in the epithelium of the terminal airway of malignant tumorous lung lesions (Anttila et al., 1993). Furthermore, a recent cohort study

* Corresponding authors at: Institute of Medical and Molecular Toxicology, Chung Shan Medical University, 110, Sec. 1, Chien-Kuo N. Road, Taichung 40203, Taiwan, ROC. Tel.: +886 4 24730022 11694; fax: +886 4 24751101.
E-mail addresses: cliff@vghtc.gov.tw (C.-P. Hsu), jlko@csmu.edu.tw (J.-L. Ko).

0378-4274/$ – see front matter © 2009 Elsevier Ireland Ltd. All rights reserved.
doi:10.1016/j.toxlet.2009.11.003

Table 1
Primer sequences specific for GST-Mu, Pi and Alpha.

Primer	Sequence 5′ → 3′	Position (bp)	Accession no.
GST-Mu-1,2,4,5-sense	5′-ATGCCCATGACACTGGGGTACTG-3′	48–70	NM_000848
GST-M1-antisense	5′-GCATATGGTTGTCCATGGTCTGG-3′	360–382	NM_000561
GST-M2-antisense	5′-GCATACGGCTGTCCATAAACTGG-3′	353–375	NM_000848
GST-M4-antisense	5′-GATTGGAGACGTCCATAGCCTGG-3′	615–637	NM_000850
GST-M5-antisense	5′-CCATGTGGTTATCCATAACCTGG-3′	376–398	NM_000851
GST-Pi-sense	5′-ATGCCGCCCTACACCGTGGTCTA-3′	30–52	NM_000852
GST-Pi-antisense	5′-ATTTGCAGCGGAGGTCCTCCACG-3′	317–339	NM_000852
GST-Alpha-sense	5′-ATGGCAGAGAAGCCCAAGCTCCA-3′	106–128	NM_000846
GST-Alpha-antisense	5′-TCATTTCACCCAAATCTGCTATA-3′	407–429	NM_000846
Beta-actin-sense	5′-TCATCACCATTGGCAATGAG-3′	813–832	NM_001101
Beta-actin-antisense	5′-CACTGTGTTGGCGTACAGGT-3′	948–967	NM_001101

indicated that the children of mothers who smoked during pregnancy had worse lung function than the children of mothers who did not smoke during pregnancy, and these children showed two alleles at multiple loci transmitted together on the same chromosome (haplotypes) of GST-M2 (Breton et al., 2009). Some reports have indicated that BPDE is a poor substrate for GST-Alph1/Alph2, but a relatively good substrate for GST-M2 (Robertson et al., 1986). GST-M2 expression may associate with lung cancer and exposure to smoke. In addition, our recent study demonstrated that the overexpression of GST-M2 transfectant cells results in reduced BPDE-induced DNA adducts by competitive ELISA and nested-PCR (Weng et al., 2005). The results indicated a role for GST-M2 activity in the prevention of DNA damage. However, the expression of GST-M2 remains undefined in non-small-cell lung carcinomas (NSCLCs).

Aberrant DNA hypermethylation of gene promoter DNA is an important epigenetic mechanism leading to downregulation and silencing of several tumor suppressor genes such as *p16*, *APC* and *MGM* (Peng et al., 2009; Schulmann et al., 2005). It can trigger the carcinogenic cascade and lead to cancer progression. In this study, our objective is to clarify the expression of GST-M2 in NSCLC patients and to determine the role of GST-M2 in protecting against DNA damage. Specifically, the aims of this study are (I) to understand the mRNA expression of GST-M2 in lung normal cell and lung cancer cell lines; (II) to analyze the mRNA expression of GST-M2 in association with clinical outcomes of early stage I and II NSCLC patients; (III) to determine the cause of the association of gene expression regulation of GST-M2 with hypermethylation or other processes and (IV) to understand the alleviation of B[a]P-induced DNA damage in NSCLCs.

2. Materials and methods

2.1. Study subjects and follow-up

Between January 2003 and August 2004, we collected lung cancer tissue specimens including cancerous tumor and adjacent normal tissues from 50 stage I and stage II NSCLC cases that underwent surgical resection in this prospective study. None of the patients received pre-operative chemotherapy or radiotherapy. Tumor staging was performed according to AJCC (6th edition) criteria (Greene, 2002). The study was conducted after human experimentation review by the IRB committee of Taichung Veterans General Hospital, and informed consent was obtained for every examined specimen. All of the patients were followed up to April 1, 2008. Tumor samples were acquired from the solid part of the mass, avoiding grossly necrotic areas. The non-tumor bearing paired tissues were acquired from the lobar edge of the resected lung with a distance of at least 5 cm from the gross tumor margin. The tissues were transferred to a fresh tube, shock frozen in liquid nitrogen and stored at −70 °C.

2.2. Cell lines and culture

Human lung cancer cells and lung cells from the American Type Culture Collection were studied. Lung cancer cell lines (adenocarcinoma cell lines A549, H1299, H1355, H23 and H460; squamous cell carcinoma cell lines CH27 and Calu-1) were cultured on Dulbecco's modified Eagle's medium (DMEM) (GIBCO, Rockville, MD). CL1-0 and its sublines CL1-5 (human lung carcinoma cell lines with different invasive and metastatic capabilities) were obtained from Dr. Pan-Chyr Yang (Chu et al., 1997). The lung normal cell lines (fibroblast cell lines MRC-5 and WI-38) were cultured on Basal medium Eagle (BME) (Sigma, Saint Louis, MI). The human bronchial epithelial cell line BEAS-2B was cultured on LHC-9 medium (GIBCO, Rockville, MD). All lung cancer cell lines were maintained at 37 °C in a 5% CO_2-humidified atmosphere on medium containing 10% fetal bovine serum (FBS; Life Technologies, Inc., Rockville, MD) and 100 ng/ml each of penicillin and streptomycin (Life Technologies, Inc.).

2.3. Isolation of RNA, RT-PCR and real-time RT-PCR analysis

DNA methylation has a long-standing relationship with gene inactivity and has been implicated in enhancement of transcriptional silencing; consistent epigenetic changes in human cancers (Jones and Baylin, 2002). H1355 cells were seeded in low density (1×10^6) 16 h before treatment. Cells were treated with de-methylation reagent 5-Aza-deoxycytidine (A3656, Sigma–Aldrich) at a final concentration of 1 and 10 μM for 96 h (Niu et al., 2009). To test the histone acetylation affect specific effect to lung cancer cell lines, we expanded the investigation to assess the effect of TSA. Cells were treated with histone deacetylase (HDAC) inhibitor, TSA (Cayman Chemical Company, Cat. No. 89730), at 0.5 μM for 24 h (Stoehlmacher et al., 2002; Xiong et al., 2005). Cells were mock-treated by adding into the medium with the same volume of DMSO alone. Total RNA was isolated using Trizol reagent (Life Technologies, Grand Island, NY), according to the manufacturer's instructions. Then, cDNA was reverse-transcribed from 2 μg total RNA used random hexamer primers and MMLV-RTase (Promega, Madison, WI). The PCR primers for cDNA are listed in Table 1. For real-time RT-PCR expression, profiling was performed using ABI PRISM 7000 real-time RT-PCR System and TaqMan gene expression probe (Applied Biosystems, Foster City, CA). A 100× dilution of resulting cDNA was used for real-time RT-PCR reactions of 40 cycles. Probes were 5′ end FAM labeled and 3′ end TAMRA labeled. Concentrations of synthesized primers and probes were optimized for each assay then real-time RT-PCR was performed in triplicate (Applied Biosystems: assays-on-gene expression products, GST-M2 probe: Hs00265266_g1; GAPDH probe: Hs99999905_m1) in a 25 μl reaction volume. GST-M2 gene expression was calculated as the ratio of signal for target gene to signal for GAPDH. Quantification was carried out using the comparative threshold cycle (C_t) method and autoclaved distilled water was used as the negative control. An optimal threshold was chosen on the basis of the 50 ng cDNA of MRC-5 signal of the same batch that was across the different plates. The relative expression levels of the target gene were calculated by $2^{-\Delta C_t}$, where $C_t = C_{t\ \text{target gene}} - C_{t\ \text{GAPDH}}$.

2.4. Comet assay analysis, chromatin isolation and Western blotting

Cells were plated onto multi-well systems at a density of 5×10^5 cells/ml culture medium. After seeding for 18 h, cells were treated with or without (8-anilino-1-naphthalene sulfonate; ANS) (200 μM) for 1 h, then exposed to B[a]P 0.2 μM for the indicated number of hours. After incubation, harvested cells were analyzed by comet assay. Suspended cells were mixed with 50 μl of low melting point agarose (0.75% concentration in PBS), distributed on slides pre-coated with low melting point agarose (0.30% concentration in PBS), and left to set on an ice tray. The slides were then immersed in ice-cold lysing solution (2.5 M NaCl, 0.1 M EDTA, 0.01 M Tris, pH 10, 1% *N*-laurylsarcosine, 1% Triton X-100, and 10% DMSO). After lyses, the slides were transferred to the electrophoresis tank in electrophoresis buffer (0.3 M NaOH, 1 mM EDTA) and kept in the dark until electrophoresis was started (20 V/cm and 150 mA for 20 min). Next, the slides were neutralized using 0.4 M Tris pH 7.5 and fixed in methanol. Subsequently, the DNA was stained with ethidium bromide for 5 min and examined under a fluorescence microscope (Nikon, E400) connected to a computerized image analysis system (Comet Assay III, Perceptive Instruments, UK). The percent DNA in tail was used as the measure of damage. At least 50 cells per experimental condition were counted from at least two experiments made in triplicate. Slides were analyzed in the absence of electrophoresis for the frequency of cells with low molecular weight (LMW) DNA. Measurements of comet parameters % DNA in the tail, tail length and tail moment were obtained. The comet percentage values of exposed cells were compared with those of unexposed cells at each experimental

point. For chromatin isolation, H1355, pcDNA/H1355 and GST-M2/H1355 transfectant cells were grown to 80% prior to exposure to B[a]P 0.2 μM for 48 h. Cells were harvested in IPB-7 buffer (triethanolamine–HCl, 20 mM, pH 7.8; NaCl, 0.7 M; NP-40, 0.5%; sodium deoxycholate 0.2%; phenylmethylsulfonyl fluoride, 1 mM; leupeptin, 1 mg/ml; pepsatin, 1 mg/ml; NaF, 1 mM; $NaVO_3$, 1 mM; trypsin inhibitor 0.1 mg/ml; aprotinin, 1 mg/ml) extraction chromatin protein. The pellet was washed three times with IPB-7 buffer, homogenized in IPB-7 by sonication and thereafter subjected to SDS-PAGE and Western blots (Al Rashid et al., 2005; Malmlof et al., 2008). For Western blot assay, equal amounts of chromatin protein from each sample were loaded onto a 15% SDS-PAGE gel and electrophoresis. Blots were probed with phosphohistone H2AX (Ser-139) antibody (Upstate Cell Signaling 05636) or total histone 3 (Abcam; ab1791). Equal loading of proteins was confirmed by staining of the blots with ECL.

2.5. Plasmids, transient transfection and reporter gene assay

The GST-M2 promoter was amplified by PCR with Taq polymerase (Ex taq, Takara) using genomic DNA from MRC-5, H1355, A549 and H1299 cell lines (50 ng) as a template, with GST-M2 promoter KpnI primer 5′-CCGGTACCGTTTTAGAGAGAGCCTTTCTTTC-3′ and GST-M2 promoter Hind III primer 5′-TTAAGCTTCACCCCGCACGCCCAGCCACACG-3′. The PCR reaction included 5-min denaturation (95 °C) followed by 35 cycles, each consisting of denaturation (95 °C, 1 min), annealing (55 °C, 1 min) and extension (72 °C, 2 min) with a final extension phase (10 min). Then, digestion was carried out with KpnI and Hind III with cloning upstream of the firefly luciferase reporter in the pGL3-Basic vector (Promega Corp.). For luciferase assay, H1355 cells (2×10^6) were seeded onto 35-mm wells. After 18 h, they were transfected with the plasmids described above (0.25 μg/μl) and β-gal (0.25 μg/μl) with Opti-MEM reduced serum medium (Invitrogen, Cat. No. 31985). After 20 min incubation, combined diluted DNA and diluted lipofectamine reagent were mixed gently and incubated at room temperature for 30 min. Then, for each transfection, the diluted complex solution was gently overlaid onto the rinsed cells. The cells were incubated with the complexes for 5 h at 37 °C. The medium was replaced with fresh, complete medium at 18 h. After carefully removing from the medium, cells were collected and transcriptional activity was assayed with luciferase assay system according to the described protocol (Promega). A plasmid expressing the bacterial β-galactosidase gene was co-transfected in each experiment to serve as internal control of transfection efficiency.

2.6. Statistical analysis

Statistical analysis was performed using the SPSS statistical software program (version 15.0, SPSS, Inc.). The relative express level of target gene in our interested variables was also classified as high or low expression groups by their median level which was calculate by $2^{-\Delta C_t}$. The χ^2 test (two tailed), Mann–Whitney test, and Wilcoxon signed-rank test were used for nonparametric pair analysis. The χ^2 test was used to determine the relationships between GST-M2 expression and various clinic pathologic characteristics including adenocarcinoma (AD) or squamous cell carcinoma (SCC), grade of cell differentiation (well, moderate or poor differentiation).

3. Results

3.1. Downregulation of GST-M2 mRNA in lung cancer cells

To identify the mRNA expression of GSTs, we analyzed the expression of six GST molecules including GST-M1, GST-M2, GST-M4, GST-M5, GST-Alpha and GST-Pi The mRNA expression profile analysis was carried out for nine lung cancer cell lines and three normal lung cell lines using RT-PCR. In Fig. 1A, among the 12 screened cell lines, GST-Alpha and GST-M5 were not detectable in any lung cells. GST-Pi was abundantly expressed in all cell lines, except in H1355 cells. GST-M1 was only expressed in some of the lung cell lines (Fig. 1A). Interestingly, we find that GST-M2 mRNA was higher expression in normal lung cell lines (MRC-5, WI-38 and BEAS-2B) than in lung cancer cell lines. GST-M2 mRNA expression was confirmed by means of real-time RT-PCR experiments (Fig. 1B). There was a more than seven-fold difference in the expression of GST-M2 transcript in normal cells and lung cancer cells. There is GST-M2 genomic expression in DNA of the lung cell lines. GST-M2 DNA was highly expressed in lung cancer and normal lung cell lines (data not shown), but its transcript was silenced in lung cancer cell lines (Fig. 1).

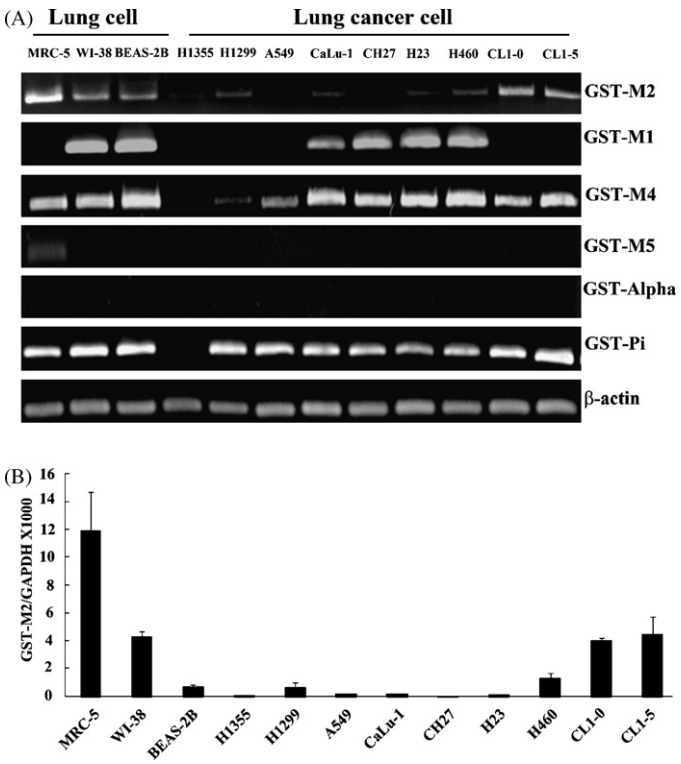

Fig. 1. GST-M2 mRNA expression in lung normal and lung tumor cell lines. (A) Representative GST-M1, GST-M2, GST-M4, GST-M5, GST-Alpha and GST-PI expressions in lung normal and lung tumor cell lines. Expression was analyzed by RT-PCR of total RNA (2 μg) amplified by RT-PCR. Equal amounts of DNA were loaded, as confirmed by the intensity of β-actin after ethidium bromide staining. (B) Real-time PCR quantification of GST-M2 by TaqMan analysis. All values have been normalized to the level of GAPDH and are the averages of three independent readings.

3.2. Association of GST-M2 expression with clinical pathology

We investigated the biological and clinic pathologic significance of GST-M2 in NSCLCs. We carried out real-time RT-PCR on lung tissue specimens of 50 NSCLC patients that underwent curative surgical resection. On the basis of the American Society of Anesthesiologists Physical Status Classification System, case patients were found to be equally fit for surgery. GST-M2 was detected with ABI 7000 specific to TagMan probe. Among the 50 NSCLC patients examined, the median of GST-M2 mRNA expression was strongly significant high in adjacent non-malignant lung tissues ($2^{-\Delta C_t}$ expression median levels = 3.73) and weakly significant low in tumor tissues ($2^{-\Delta C_t}$ expression median levels = 1.33); ($p = 0.016$, Wilcoxon signed-rank test) (Fig. 2). Our data show that loss of mRNA expression of GST-M2 in lung tumor tissues was in agreement with the pattern in lung tumor cell lines (Fig. 1A). There were significant associations between clinical pathological factors and the median of mRNA expression in GST-M2 ($p < 0.05$, Wilcoxon signed-rank test) such as patients age (≧67 years), male gender, *T* value 1,2, N_0, poor cell differentiation (Table 2). These results indicate that the mRNA expression of GST-M2 signature is dependent on these clinical parameters in lung cancer. Then, we classified cases into GST-M2 high and low expression groups. The cutoff value for patient stratification was determined by the median of total mRNA expression of all tumor tissues. For example, a case was classified as high if the mRNA expression of GST-M2 coefficient was ≧3.73 ($n = 25$); otherwise, it was classified as low (mRNA expression levels <3.73; $n = 25$). We applied the correlation of the high and low expressions of GST-M2 to the overall survival times of NSCLC patients. Most of the variables were not significantly associated with high expression of GST-M2, except for gender (male), cell dif-

Table 2
Characteristics of patients with NSCLC in relation to expression of the GST M2 gene.

Characteristics	*n* (%)	GST-M2 median (min–max)		
		Adjacent non-malignant lung tissues	Tumor tissues	*p*-value
Age (year[a])				
<67	24 (48)	4.81 (0.04–49.77)	4.64 (0.04–79.55)	0.54
≧67	26 (52)	2.61 (0.30–95.61)	0.95 (0.06–73.48)	0.01**
Gender				
Male	37 (74)	2.63 (0.04–95.61)	1.55 (0.04–75.99)	0.04*
Female	13 (26)	6.52 (0.30–49.77)	0.97 (0.12–71.77)	0.27
Histology				
AD	31 (62)	4.02 (0.04–95.61)	1.11 (0.04–79.55)	0.07
SQ	19 (38)	2.63 (0.55–95.61)	2.36 (0.04–38.97)	0.17
Stage				
I	33 (66)	4.02 (0.04–95.61)	1.11 (0.04–79.55)	0.08
II	17 (34)	2.90 (0.42–49.77)	1.55 (0.12–38.97)	0.14
T value				
1, 2	40 (80)	3.98 (0.04–95.61)	1.74 (0.04–79.55)	0.04*
3	10 (20)	2.59 (0.42–49.77)	1.32 (0.12–38.97)	0.34
N value				
0	43 (86)	3.95 (0.04–95.61)	1.11 (0.04–79.55)	0.03*
1	7 (14)	3.50 (1.39–33.14)	2.36 (0.27–9.95)	0.45
Cell differentiation				
Well and moderate	26 (52)	3.49 (0.30–95.61)	2.58 (0.06–79.55)	0.56
Poor	24 (48)	4.13 (0.04–49.77)	0.95 (0.04–38.97)	0.007**

AD, adenocarcinoma; SCC, squamous cell carcinoma. Wilcoxon signed-rank test.
[a] The median age of the 50 patients is 67 years.
* $p < 0.05$.
** $p < 0.01$.

ferentiation (poor) on Kaplan–Meier analysis (data not shown). Our findings are important as they provide clues to the trends underlying that loss the mRNA expression in GST-M2 in tumor tissues and tumor cell lines relationship.

3.3. DNA hypermethylation of GST-M2 promoter correlated with reduced mRNA expression

As shown in Fig. 1A, there is GST-M2 mRNA expression loss in lung cancer cell line. We thought that if different base in promoter region of GST-M2 could affect the expression between high and low GST-M2 expression cells. In order to determine the cause of this GST-M2 mRNA expression loss, we first clarified the occurrence of genomic DNA sequence changes in the promoter region of GST-M2. Analysis of the promoter regions of GST-M2 gene indicated −387 to +244 bp relative to the transcription start site. We identified one base mutation at +128, downstream of the GST-M2 gene transcription start code (Fig. 3A). Lung cancer cell lines (H1355, H1299 and A549) have point mutation T base substitution at +128 (mutant type) in contrast to lung normal cell line that has C base (wild type). To identify the core promoter at different base at +128 bp essential for transcriptional activation, 5′ mutation type of the fragments was prepared and tested by luciferase assay. Transcriptional activity in H1355 cell line with wild type or mutant type exhibited the same activity (Fig. 3B). Moreover, the transcriptional activity increased with more DNA transfection (0.25 and 0.5 μg). Our findings suggest that these sequences change at +128 bp do not affect the activity of the promoter of GST-M2. The point mutation at +128 GGC (Gly) to GGT (Gly) was silent mutation. Therefore, downregulated GST-M2 expression was not due to the mutation in promoter region.

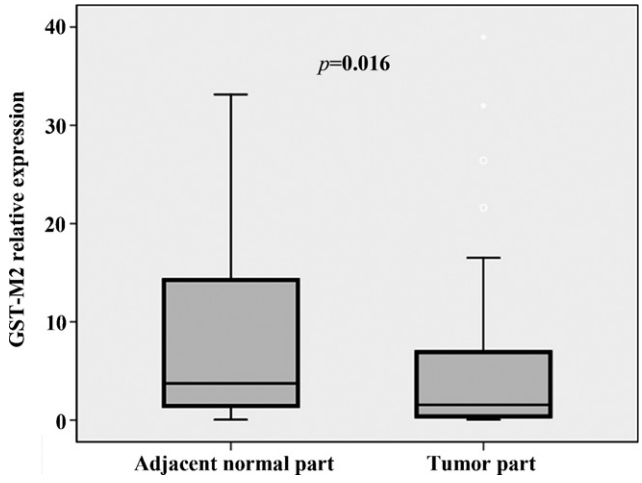

Fig. 2. Comparison of the GST-M2 mRNA expression levels in lung tumor part and adjacent normal part. GST-M2 expression level for the total 50 NSCLC patients primary tumor part was compared with its paired adjacent normal part. The mRNA expression of GST-M2 level was quantitated by semiquantitative real-time PCR. Quantitative ratio is defined as the ratio of the fluorescence emission intensity values for the PCR products of the GST-M2 gene to those of PCR products. The GST-M2 mRNA expression levels were analyzed using the Wilcoxon rank sum test to determine the statistical significance. A *p* value of ≦0.05 was considered statistically significant.

Next, we examined the expression of GST-M2 after treatment with de-methylation reagent 5-Aza in NSCLC cell line. Our data show that GST-M2 mRNA expression is dependent on 5-Aza (10 μM) treatment and is restored in the H1355 cells (Fig. 4A). We confirmed the mean of difference analysis by real-time RT-PCR (**$p < 0.01$) (Fig. 4B). These data suggest that silence of GST-M2 mRNA expression is associated with promoter DNA hypermethylation. Our data also showed that HDAC inhibitor-TSA at 0.5 μM is not effective in restore the mRNA expression of GST-M2 in lung cancer cell lines. E-cadherin expression was not detected due to DNA hypermethylation and acetylation. Therefore, E-cadherin was shown as positive control for treatment with TSA (Fig. 4A; lane 5). This suggests that histone modifications are not involved in regulating the mRNA expression of GST-M2. As for the model, we also confirmed 5-Aza and 5-Aza (10 μM)/TSA (0.1 or 0.5 μM) treatments in lung cancer cell line analysis by Western blot. There

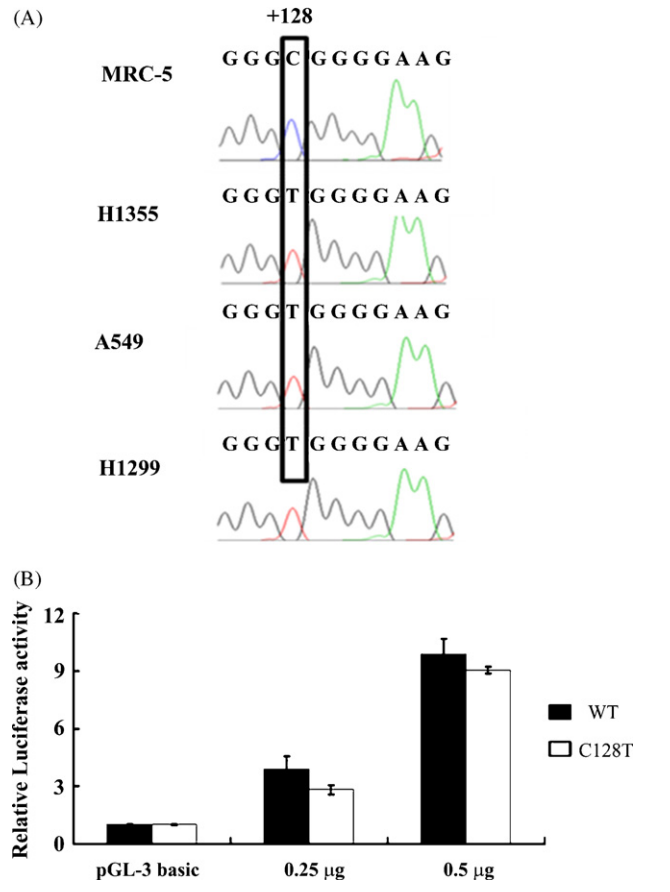

Fig. 3. Promoter sequences of GST-M2 in MRC-5, H1355, A549 and H1299 cells. (A) The point mutation C to T of GST-M2 promoter located at +128 bp upstream of the GST-M2 transcription start site were identified in H1355, A549 and H1299 lung tumor cell lines. (B) On luciferase activity assay in H1355 cells, the relative measured luciferase levels are depicted on a bar graph, whereby pGL-3 luciferase reporter plasmids containing either C 128 T sequence or wild-type sequence are co-transfected with pGL-3 basic. Each value is the average of at least three independent experiments and the error bars represent the standard deviation.

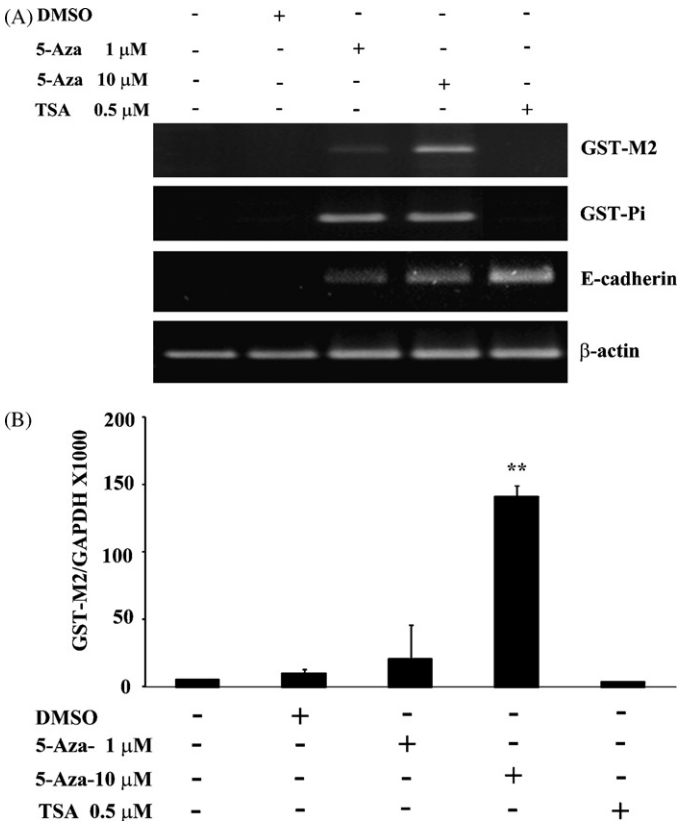

Fig. 4. Transcription re-expression of the methylated genes following 5-aza-2′-deoxycytidine (5-Aza) and trichostatin-A (Stoehlmacher et al., 2002) treatments. (A) The H1355 cell line was treated with 1, 10 μM 5-Aza for 96 h or 0.5 μM TSA for 24 h. RT-PCR analysis of equal amounts of cDNA from cells demonstrate upregulation of the GST-M2 proteins in treated cells as compared with control. β-actin is shown as a loading control. The GST-PI is shown as positive control. (B) Real-time RT-PCR analysis confirms the same model. The mRNA expression was calculated as the relative expression as compared to GAPDH. $^{**}p < 0.01$ vs nontreated control.

was no effect on translation of GST-M2 proteins (data not shown). Together, these data suggest that loss mRNA expression of GST-M2 in lung cancer cell lines was through hypermethylation of GST-M2 promoter, but not acetylation of histone, or promoter mutation.

3.4. Alleviation of benzo[a]pyrene-induced DNA damage by GST-M2 in lung cancer cells

To evaluate the protective effect of GST-M2 against B[a]P-induced DNA damage in lung cancer cell line, comet assay and γ-H2AX were carried out. The extent of DNA strands break (measured as tail length, the percentage of migrated DNA and olive tail moment) was determined by scoring cells. In our previously study, we construct the GST-M2 mRNA overexpression in H1355 cell lines (Weng et al., 2005). H1355 cells treated with 0.2 μM B[a]P showed significant increases in DNA strand breaks. When damaged initially, DNA fragments became free to migrate in the electric field toward the anode and the tail length increased (Fig. 5A). There were significant related-time increases in DNA damage at 12, 24 and 48 h. We analyzed the DNA tail moment with 0.2 μM B[a]P at 0, 12, 24 and 48 h in H1355 cells (Fig. 5B black columns), and significant increases were found time-dependent (from 0.6 ± 0.45 μm to 12.1 ± 2.7 μm, 28.3 ± 5.9 μm and 35.4 ± 3.6 μm). Subsequently, in H1355 cells with GST-M2 mRNA overexpression treated with B[a]P there were statistically significant decreases in DNA damage (Fig. 5B hatched columns) at 0, 12, 24 and 48 h, most notably alleviation of DNA strand break (from 1.53 ± 0.21 μm to 4.0 ± 0.5 μm, 5.6 ± 0.6 μm and 14.2 ± 1.39 μm) (a, compare with pcDNA/H1355, $p < 0.01$, Student's t-test). We therefore examined DNA fragmentation after pre-treatment with ANS at 200 μM, a high binding capacity for non-substrate compound. The GST-M2 activity could be inhibited by ANS in vitro and in vivo (Mosebi et al., 2003). This caused a significant increase in DNA damage at 12, 24 and 48 h. (Fig. 5B rhombus columns) (from 12.1 ± 0.21 μm to 18.8 ± 1.8 μm and 25.6 ± 1.0 μm) (b, compare with GST-M2 transfectants/H1355, $p < 0.05$, Student's t-test).These results indicated that B[a]P-induced DNA strand breakage is time-dependent in lung cancer cells.

Upon DNA double-strand break (DSB) induction in mammals, H2AX become rapidly phosphorylated at serine 139 and termed to form γ-H2AX that is easily identified and serves as a sensitive indicator of DNA DSB formation (Dickey et al., 2009). Therefore, induction of γ-H2AX is found following exposure of cells to suspected DNA-damaging compounds such as cigarette smoke (Albino et al., 2004), polycyclic aromatic compounds, dinitrobenzo[e]pyrene (Mattsson et al., 2009). We detected γ-H2AX chromatin protein on Western blotting at sites flanking DSBs. GST-M2 overexpression in H1355 cells significantly alleviates DNA double-strand breaks (Fig. 6). These results indicate that GST-M2 overexpression can be significantly effective in protecting against B[a]P-induced DNA damage in lung cancer cells.

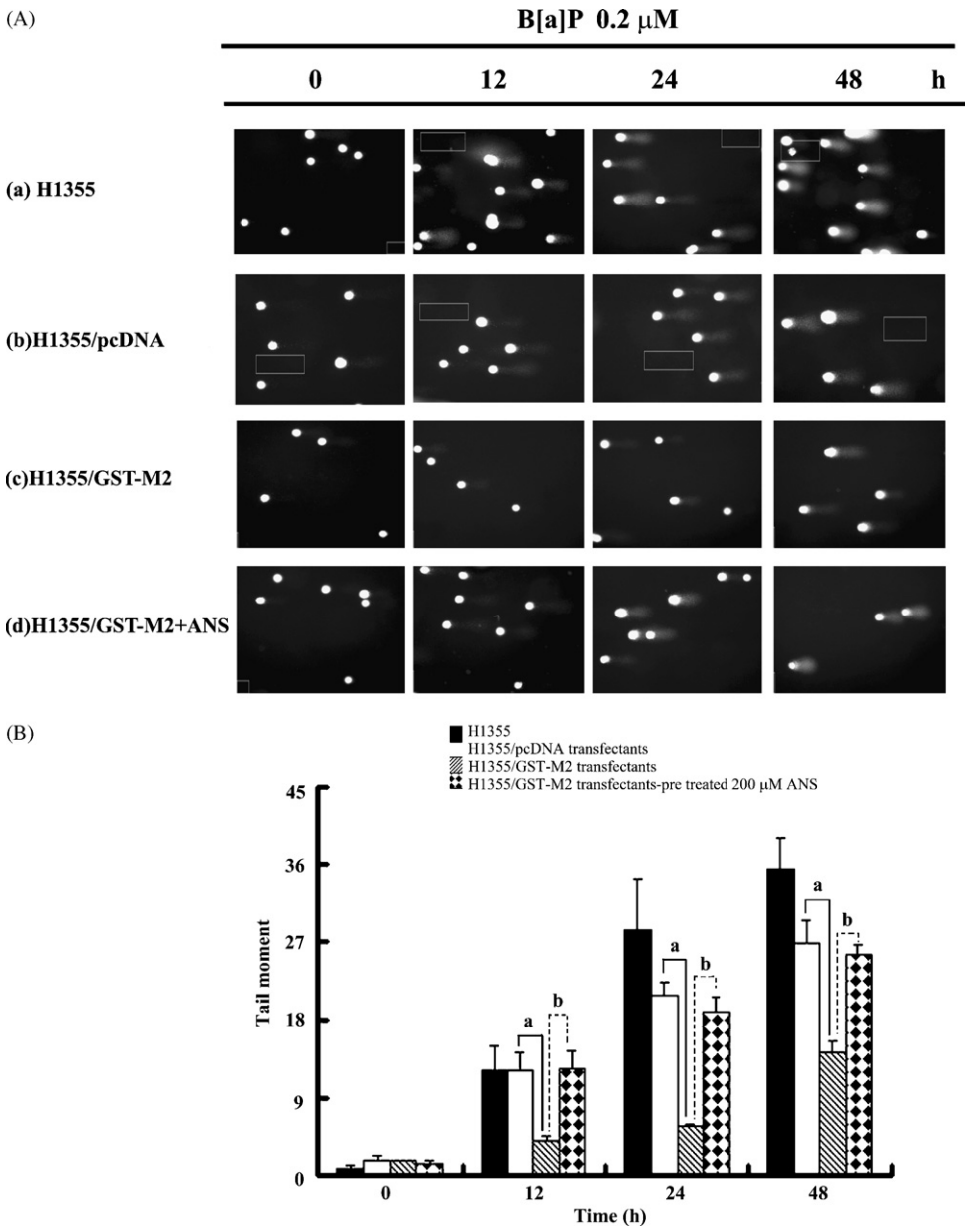

Fig. 5. B[a]P induced DNA damage as evidenced by tail moment. (A) Mean tail moments of H1355 cells, pcDNA/H1355 transfectant cells and GST-M2/H1355 transfectant cells pretreated with ANS (200 μM) 1 h prior to incubation with B[a]P 0.2 μM for 12, 24 and 48 h. (a) $p < 0.01$ for comparisons of GST-M2/H1355 transfectants and pcDNA/H1355 transfectant cells. (b) $p < 0.05$ for comparisons of GST-M2/H1355 transfectants pretreated with 200 μM ANS and GST-M2/H1355 transfectants. The tail moments were calculated by determining the surface area of the same range. (B) The tail moment = %DNA in tail × tail length.

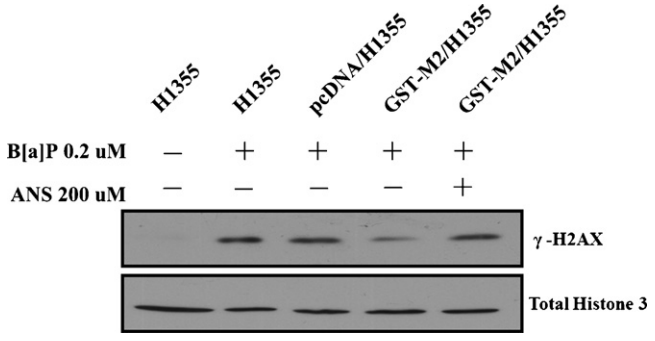

Fig. 6. Western blot analysis of the γ-H2AX response exposure to B[a]P in H1355, pcDNA/H1355 and GST-M2/H1355 transfectant cells. Cells were treated for 48 h with B[a]P 0.2 μM or ANS 200 μM (non-substrate ligand for GST-M2 inhibitor) and analyzed for γ-H2AX chromatin protein expression by Western blot. Total Histone 3 is shown as a loading control.

4. Discussion

Our findings suggest that the significant loss GST-M2 mRNA expression was in lung cancer cell lines, not in lung normal cell lines (Fig. 1A). GST-M2 mRNA expression undergoes de-methylation and restore after exposure to de-methylation agent 5-Aza-2′-deoxycytidine in lung cancer cells (Fig. 4A). Loss of GST-M2 in lung cancer cells causes DNA damage upon exposure to B[a]P (Figs. 5 and 6). Therefore, the data support our hypothesis that the hypermethylation leading to silencing GST-M2 expression in lung cancer cells and become more sensitive to long-term exposure to carcinogenic agents, such as B[a]P and PAH.

In general, GST-M2 mRNA expression was higher in lung normal cell lines (MRC-5, WI-38 and BEAS-2B) than lung cancer cell lines using RT-PCR. It looks like that GST-M2 expression was higher in lung fibroblasts than in epithelial cells (Fig. 1). The data suggested that GST-M2 expression might be higher in stroma or normal

parts than in epithelial cells or tumor parts. Using real-time RT-PCR, we found a significant association for GST-M2 expression between the tumors and adjacent non-malignant lung tissues ($p = 0.016$) in patients with NSCLCs. There are high levels of GST-M2 in adjacent non-malignant lung tissues but low or absent levels of GST-M2 in tumor tissues (Fig. 2). Aberrant DNA hypermethylation of gene promoter regions is an epigenetic mechanism leading to silencing of tumor suppressor genes in many human cancers (Peng et al., 2009). Downregulation of GST-M2 is mediated through aberrant hypermethylation in lung cancer cell lines (Fig. 4). We consider that there have a higher proportion of GST-M2 hypermethylation in NSCLC patients.

We observed that B[a]P-induced DNA strand breakage is time-dependent in H1355 cells and the effect is most severe at 24 h (Fig. 5). These findings are in agreement with previous reports which measured DNA breaks in alveolar macrophages, lung cells, peripheral lymphocytes of Sprague-Dawley rats, exposed to a single dose of B[a]P by endotracheal administration (Garry et al., 2003). H2AX is a key regulator of the DNA damage response, because H2AX plays an essential role in the recruitment and accumulation of DNA repair proteins to sites of DSB damage (like replication fork collapse) (Furuta et al., 2003), and leads to the DNA repair response start. Those proteins include 53BP1, MDC1, RAD51, BRCA1, and the MRE11/RAD50/NBS1 (Dickey et al., 2009). The chromatin remodeling complex TIP60-UBC13, which also participates in DNA repair, is recruited to the DSB site by γ-H2AX (Ikura et al., 2007). In our hypothesis that the hypermethylation leading to silencing GST-M2 expression in lung cancer cells became more sensitive to long-term exposure to carcinogenic agents, such as B[a]P and PAH. Thus, GST-M2 prevented BPDE-DNA adducts and γ-H2AX formation did not enhance DNA repair capability for BPDE-DNA adducts. Thus, hypermethylation of tumor suppressor genes forms the basis for development of biomarkers for early detection of lung cancer (Sidransky, 2002). One might conceptualize that biomarkers show high levels of methylation in tumor but very low methylation in adjacent non-malignant lung tissues (Shivapurkar et al., 2007). We are confident that the hypothesis of GST-M2 hypermethylation in NSCLC tissues is supported.

Most studied of the GSTs is GST-M1, which is only expressed in 50% of the population (Seidegard et al., 1988). Similarly, the expression of GST-M1 was inconsistent in our study (Fig. 1A). A study indicated that the proportion of the GST-M1 gene deletion genotype significantly increased in lung cancer patients in Russia (81%). Next, we assessed expression by quantitative real-time PCR in 50 patients. GST-M1 was the least expressed within adjacent non-malignant parts or lung tumor tissues (data not shown). Another study indicated that on immunostaining GST-M1 expression went from being absent to being weak in the bronchial cells of human lung tissues (Anttila et al., 1993). Although the GST-M1 and GST-M2 genes are closely related, sharing 97% of their nucleotides (Konig-Greger et al., 2004), GST-Mu class is highly diverse.

In conclusion, our data demonstrated a loss of expression of GST-M2 in tumor part of NSCLCs and hypermethylation mediated GST-M2 gene silence. This study provides new insight into the molecular mechanism of GST-M2 expression. Moreover, delineating the alleviation of DNA damage induced by B[a]P manifests a major detoxification role for GST-M2. Thus, quantitative analysis of GST-M2 for levels of methylation within its promoter sequences in NSCLCs appears to be a promising marker in our future study.

Acknowledgment

This study was supported by the National Science Council, Taiwan, ROC (NSC-95-2311-B040-003 and NSC96-2314-B040-014-MY3)

References

Al Rashid, S.T., Dellaire, G., Cuddihy, A., Jalali, F., Vaid, M., Coackley, C., Folkard, M., Xu, Y., Chen, B.P., Chen, D.J., Lilge, L., Prise, K.M., Bazett Jones, D.P., Bristow, R.G., 2005. Evidence for the direct binding of phosphorylated p53 to sites of DNA breaks in vivo. Cancer Res. 65, 10810–10821.

Albino, A.P., Huang, X., Jorgensen, E., Yang, J., Gietl, D., Traganos, F., Darzynkiewicz, Z., 2004. Induction of H2AX phosphorylation in pulmonary cells by tobacco smoke: a new assay for carcinogens. Cell Cycle 3, 1062–1068.

Alexandrov, K., Cascorbi, I., Rojas, M., Bouvier, G., Kriek, E., Bartsch, H., 2002. CYP1A1 and GSTM1 genotypes affect benzo[a]pyrene DNA adducts in smokers' lung: comparison with aromatic/hydrophobic adduct formation. Carcinogenesis 23, 1969–1977.

Alexandrov, K., Rojas, M., Rolando, C., 2006. DNA damage by benzo(a)pyrene in human cells is increased by cigarette smoke and decreased by a filter containing rosemary extract, which lowers free radicals. Cancer Res. 66, 11938–11945.

Anttila, S., Hirvonen, A., Vainio, H., Husgafvel-Pursiainen, K., Hayes, J.D., Ketterer, B., 1993. Immunohistochemical localization of glutathione S-transferases in human lung. Cancer Res. 53, 5643–5648.

Breton, C.V., Vora, H., Salam, M.T., Islam, T., Wenten, M., Gauderman, W.J., Van Den Berg, D., Berhane, K., Peters, J.M., Gilliland, F.D., 2009. Variation in the GST Mu locus and tobacco smoke exposure as determinants of childhood lung function. Am. J. Respir. Crit. Care Med..

Castro, V.M., Soderstrom, M., Carlberg, I., Widersten, M., Platz, A., Mannervik, B., 1990. Differences among human tumor cell lines in the expression of glutathione transferases and other glutathione-linked enzymes. Carcinogenesis 11, 1569–1576.

Chu, Y.W., Yang, P.C., Yang, S.C., Shyu, Y.C., Hendrix, M.J., Wu, R., Wu, C.W., 1997. Selection of invasive and metastatic subpopulations from a human lung adenocarcinoma cell line. Am. J. Respir. Cell. Mol. Biol. 17, 353–360.

Dickey, J.S., Redon, C.E., Nakamura, A.J., Baird, B.J., Sedelnikova, O.A., Bonner, W.M., 2009. H2AX: functional roles and potential applications. Chromosoma 118, 683–692.

Furuta, T., Takemura, H., Liao, Z.Y., Aune, G.J., Redon, C., Sedelnikova, O.A., Pilch, D.R., Rogakou, E.P., Celeste, A., Chen, H.T., Nussenzweig, A., Aladjem, M.I., Bonner, W.M., Pommier, Y., 2003. Phosphorylation of histone H2AX and activation of Mre11, Rad50, and Nbs1 in response to replication-dependent DNA double-strand breaks induced by mammalian DNA topoisomerase I cleavage complexes. J. Biol. Chem. 278, 20303–20312.

Garry, S., Nesslany, F., Aliouat, E., Haguenoer, J.M., Marzin, D., 2003. Assessment of genotoxic effect of benzo[a]pyrene in endotracheally treated rat using the comet assay. Mutat. Res. 534, 33–43.

Greene, F.L., 2002. The American Joint Committee on cancer: updating the strategies in cancer staging. Bull. Am. Coll. Surg. 87, 13–15.

Hayes, J.D., Pulford, D.J., 1995. The glutathione S-transferase supergene family: regulation of GST and the contribution of the isoenzymes to cancer chemoprotection and drug resistance. Crit. Rev. Biochem. Mol. Biol. 30, 445–600.

Ikura, T., Tashiro, S., Kakino, A., Shima, H., Jacob, N., Amunugama, R., Yoder, K., Izumi, S., Kuraoka, I., Tanaka, K., Kimura, H., Ikura, M., Nishikubo, S., Ito, T., Muto, A., Miyagawa, K., Takeda, S., Fishel, R., Igarashi, K., Kamiya, K., 2007. DNA damage-dependent acetylation and ubiquitination of H2AX enhances chromatin dynamics. Mol. Cell. Biol. 27, 7028–7040.

Jones, P.A., Baylin, S.B., 2002. The fundamental role of epigenetic events in cancer. Nat. Rev. Genet. 3, 415–428.

Kearns, P.R., Chrzanowska-Lightowlers, Z.M., Pieters, R., Veerman, A., Hall, A.G., 2003. Mu class glutathione S-transferase mRNA isoform expression in acute lymphoblastic leukaemia. Br. J. Haematol. 120, 80–88.

Kelley, M.J., Glaser, E.M., Herndon 2nd, J.E., Becker, F., Bhagat, R., Zhang, Y.J., Santella, R.M., Carmella, S.G., Hecht, S.S., Gallot, L., Schilder, L., Crowell, J.A., Perloff, M., Folz, R.J., Bergan, R.C., 2005. Safety and efficacy of weekly oral oltipraz in chronic smokers. Cancer Epidemiol. Biomarkers Prev. 14, 892–899.

Konig-Greger, D., Riechelmann, H., Wittich, U., Gronau, S., 2004. Genotype and phenotype of glutathione-S-transferase in patients with head and neck carcinoma. Otolaryngol. Head Neck Surg. 130, 718–725.

Malmlof, M., Paajarvi, G., Hogberg, J., Stenius, U., 2008. Mdm2 as a sensitive and mechanistically informative marker for genotoxicity induced by benzo[a]pyrene and dibenzo[*a*,l]pyrene. Toxicol. Sci. 102, 232–240.

Mannervik, B., Castro, V.M., Danielson, U.H., Tahir, M.K., Hansson, J., Ringborg, U., 1987. Expression of class Pi glutathione transferase in human malignant melanoma cells. Carcinogenesis 8, 1929–1932.

Matthias, C., Jahnke, V., Hand, P., Fryer, A.A., Strange, R.C., 1999. Immunohistologic and molecular genetic studies of the effect of glutathione-S-transferases on the development of squamous epithelial carcinomas in the area of the head-neck. Laryngorhinootologie 78, 182–188.

Mattsson, A., Lundstedt, S., Stenius, U., 2009. Exposure of HepG2 cells to low levels of PAH-containing extracts from contaminated soils results in unpredictable genotoxic stress responses. Environ. Mol. Mutagen. 50, 337–348.

Mosebi, S., Sayed, Y., Burke, J., Dirr, H.W., 2003. Residue 219 impacts on the dynamics of the C-terminal region in glutathione transferase A1-1: implications for stability and catalytic and ligandin functions. Biochemistry 42, 15326–15332.

Niu, D., Zhang, J., Ren, Y., Feng, H., Chen, W.N., 2009. HBx genotype D represses GSTP1 expression and increases the oxidative level and apoptosis in HepG2 cells. Mol. Oncol. 3, 67–76.

Orlow, I., Park, B.J., Mujumdar, U., Patel, H., Siu-Lau, P., Clas, B.A., Downey, R., Flores, R., Bains, M., Rizk, N., Dominguez, G., Jani, J., Berwick, M., Begg, C.B., Kris, M.G.,

Rusch, V.W., 2008. DNA damage and repair capacity in patients with lung cancer: prediction of multiple primary tumors. J. Clin. Oncol. 26, 3560–3566.
Peng, D.F., Razvi, M., Chen, H., Washington, K., Roessner, A., Schneider-Stock, R., El-Rifai, W., 2009. DNA hypermethylation regulates the expression of members of the Mu-class glutathione S-transferases and glutathione peroxidases in Barrett's adenocarcinoma. Gut 58, 5–15.
Robertson, I.G., Guthenberg, C., Mannervik, B., Jernstrom, B., 1986. Differences in stereoselectivity and catalytic efficiency of three human glutathione transferases in the conjugation of glutathione with 7 beta,8 alpha-dihydroxy-9 alpha,10 alpha-oxy-7,8,9,10-tetrahydrobenzo(a)pyrene. Cancer Res. 46, 2220–2224.
Rojas, M., Marie, B., Vignaud, J.M., Martinet, N., Siat, J., Grosdidier, G., Cascorbi, I., Alexandrov, K., 2004. High DNA damage by benzo[a]pyrene 7,8-diol-9,10-epoxide in bronchial epithelial cells from patients with lung cancer: comparison with lung parenchyma. Cancer Lett. 207, 157–163.
Schulmann, K., Sterian, A., Berki, A., Yin, J., Sato, F., Xu, Y., Olaru, A., Wang, S., Mori, Y., Deacu, E., Hamilton, J., Kan, T., Krasna, M.J., Beer, D.G., Pepe, M.S., Abraham, J.M., Feng, Z., Schmiegel, W., Greenwald, B.D., Meltzer, S.J., 2005. Inactivation of p16, RUNX3, and HPP1 occurs early in Barrett's-associated neoplastic progression and predicts progression risk. Oncogene 24, 4138–4148.
Seidegard, J., Vorachek, W.R., Pero, R.W., Pearson, W.R., 1988. Hereditary differences in the expression of the human glutathione transferase active on trans-stilbene oxide are due to a gene deletion. Proc. Natl. Acad. Sci. U.S.A. 85, 7293–7297.
Shea, T.C., Kelley, S.L., Henner, W.D., 1988. Identification of an anionic form of glutathione transferase present in many human tumors and human tumor cell lines. Cancer Res. 48, 527–533.
Shivapurkar, N., Stastny, V., Suzuki, M., Wistuba, I.I., Li, L., Zheng, Y., Feng, Z., Hol, B., Prinsen, C., Thunnissen, F.B., Gazdar, A.F., 2007. Application of a methylation gene panel by quantitative PCR for lung cancers. Cancer Lett. 247, 56–71.
Sidransky, D., 2002. Emerging molecular markers of cancer. Nat. Rev. Cancer 2, 210–219.
Stoehlmacher, J., Park, D.J., Zhang, W., Groshen, S., Tsao-Wei, D.D., Yu, M.C., Lenz, H.J., 2002. Association between glutathione S-transferase P1, T1, and M1 genetic polymorphism and survival of patients with metastatic colorectal cancer. J. Natl. Cancer Inst. 94, 936–942.
Sundberg, K., Dreij, K., Seidel, A., Jernstrom, B., 2002. Glutathione conjugation and DNA adduct formation of dibenzo[a,l]pyrene and benzo[a]pyrene diol epoxides in V79 cells stably expressing different human glutathione transferases. Chem. Res. Toxicol. 15, 170–179.
Tsuchida, S., Maki, T., Sato, K., 1990. Purification and characterization of glutathione transferases with an activity toward nitroglycerin from human aorta and heart. Multiplicity of the human class Mu forms. J. Biol. Chem. 265, 7150–7157.
Weng, M.W., Hsiao, Y.M., Chiou, H.L., Yang, S.F., Hsieh, Y.S., Cheng, Y.W., Yang, C.H., Ko, J.L., 2005. Alleviation of benzo[a]pyrene-diolepoxide-DNA damage in human lung carcinoma by glutathione S-transferase M2. DNA Repair (Amst) 4, 493–502.
Xiong, Y., Dowdy, S.C., Podratz, K.C., Jin, F., Attewell, J.R., Eberhardt, N.L., Jiang, S.W., 2005. Histone deacetylase inhibitors decrease DNA methyltransferase-3B messenger RNA stability and down-regulate de novo DNA methyltransferase activity in human endometrial cells. Cancer Res. 65, 2684–2689.